Identification and Characterization of the Product Release Steps within the Catalytic Cycle of Protochlorophyllide Oxidoreductase†

Derren J. Heyes* and C. Neil Hunter

Robert Hill Institute for Photosynthesis and Krebs Institute for Biomolecular Research, Department of Molecular Biology and Biotechnology, University of Sheffield, Sheffield S10 2TN, United Kingdom

Received March 2, 2004; Revised Manuscript Received April 19, 2004

ABSTRACT: The chlorophyll biosynthetic enzyme protochlorophyllide reductase (POR) catalyzes the reduction of protochlorophyllide (Pchlide) into chlorophyllide (Chlide) with reduced nicotinamide adenine dinucleotide phosphate (NADPH) as a cofactor. POR is a light-driven enzyme, which has provided a unique opportunity to trap intermediates and identify different steps in the reaction pathway by initiating catalysis with illumination at low temperatures. In the present work we have used a thermophilic form of POR, which has an increased conformational rigidity at comparable temperatures, to dissect and study the final stages of the reaction where protein dynamics are proposed to play an important role in catalysis. Low-temperature fluorescence and absorbance measurements have been used to demonstrate that the reaction pathway for this enzyme consists of two additional "dark" steps, which have not been detected in previous studies. Product binding studies were used to show that spectroscopically distinct Chlide species could be observed and were dependent on whether the NADPH or $NADP^+$ cofactor was present. As a result we have been able to identify the intermediates that are observed during the latter stages of the POR catalytic cycle and have shown that they are formed via a series of ordered product release and cofactor binding events. These events involve release of $NADP^+$ from the enzyme and its replacement by NADPH, before release of the Chlide product has taken place. Following release of Chlide, the subsequent binding of Pchlide allows the next catalytic cycle to proceed.

The light-driven enzyme NADPH:protochlorophyllide oxidoreductase (POR;[1] EC 1.3.1.33) catalyzes the reduction of the C17−C18 double bond of the *D*-ring of protochlorophyllide (Pchlide) to produce chlorophyllide (Chlide) (*1*). As a result of this requirement for light, the reaction is an important regulatory step in the chlorophyll biosynthetic pathway and subsequent assembly of the photosynthetic apparatus (*2*). In addition to POR, nonflowering land plants, algae, and cyanobacteria possess a light-independent Pchlide reductase, which consists of three separate subunits and allows these organisms to produce Chlide in the dark (*3*).

The reaction catalyzed by POR has been extensively studied and a lot of progress has been made in elucidating the catalytic mechanism. By using 4*R* and 4*S* ^{3}H-radiolabeled isomers of NADPH, it has been shown that the hydride is transferred from the *pro-S* face of the nicotinamide ring to the C17 position of the Pchlide molecule (*4*, *5*). A conserved Tyr residue has been proposed to donate a proton to the C18 position whereas the close proximity of a conserved Lys residue is thought to be necessary to lower the apparent pK_a of the phenolic group of the Tyr, allowing deprotonation to occur (*6*). In addition, changes to the central Mg atom (*7*) and to the structure of the isocyclic ring of the Pchlide molecule lead to POR inactivity (*8*), suggesting that these structural elements are also important for the interaction of the pigment with the enzyme.

POR has also been shown to be a member of the large RED superfamily of enzymes (reductases, epimerases, dehydrogenases) (*6*, *9*), which catalyze NADP(H)- or NAD(H)-dependent reactions involving hydride and proton transfers (*10*). They have many structural features in common, including conserved cofactor binding domains and the conserved catalytic Tyr and Lys residues, and as a result a homology model of POR has been constructed with this family as a template (*11*). As POR is light-driven, this provides unique experimental opportunities that are unavailable for the majority of enzymes. The active enzyme−substrate complex can be formed in the dark, prior to catalysis, which allows intermediates in the reaction pathway to be observed by initiating catalysis with illumination at low temperatures. Therefore, this makes POR an attractive model for studying the mechanism of this family and more generally biological proton and hydride transfers.

The recent advent of heterologous expression systems has provided an excellent opportunity to study the reaction in greater detail (*12*−*16*). We have previously used low-temperature spectroscopy to identify three distinct steps in the reaction pathway for POR from the cyanobacterium *Synechocystis*, one that is light-driven followed by two "dark"

† This work was supported by the Joint Infrastructure Fund and the Biotechnology and Biological Sciences Research Council, U.K.

* To whom correspondence should be addressed: Department of Molecular Biology and Biotechnology, University of Sheffield, Firth Court, Western Bank, Sheffield S10 2TN, U.K. Telephone: +44 (0)-114 2224240. Fax: +44 (0)114 2222711. E-mail: d.j.heyes@shef.ac.uk.

[1] Abbreviations: Pchlide, protochlorophyllide; Chlide, chlorophyllide; POR, light-dependent NADPH:protochlorophyllide oxidoreductase; NADPH ($NADP^+$), reduced (oxidized) nicotinamide adenine dinucleotide phosphate; fwhm, full width at half-maximum; RED, reductases, epimerases, dehydrogenases; PCR, polymerase chain reaction; DTT, dithiothreitol.

10.1021/bi049576h CCC: $27.50
Published on Web 06/03/2004

reactions. The initial photochemical step, which can occur below 200 K, involves the formation of a nonfluorescent intermediate with a broad absorbance band at 696 nm (*17*). This species is then converted into a new intermediate that has an absorbance maximum at 681 nm, and during the second dark step this state gradually blue-shifts to yield the product, Chlide (*18*). Although the exact molecular nature of these intermediates is currently unknown, the two dark steps can only occur close to or above the glass transition temperature of proteins, implying a role for domain movements and/or reorganization of the protein for these stages of the catalytic mechanism. The reaction catalyzed by POR has also been followed in real time after initiation of catalysis with a 50 fs laser pulse. The study revealed that the reaction, and hence the associated protein motions, can proceed on an ultrafast time scale (*19*).

In the present work POR from the thermophilic cyanobacterium *Thermosynechococcus elongatus* BP-1 has been analyzed by using fluorescence and absorbance spectral measurements at 77 K. The use of a thermophilic version of POR provides the opportunity to follow the reaction over a much wider temperature range. In addition, thermophilic enzymes are generally barely active at room temperature when compared to their mesophilic counterparts. This loss of activity is caused by the reduced conformational flexibility of thermophilic enzymes at lower temperatures (*20*−*22*). Hence, thermophilic POR should be an ideal model system to follow at accessible temperatures the latter stages of the reaction, where protein motions play an important role. Consequently, we have shown that the dark reactions of the thermophilic enzyme consist of two additional steps, which have not been detected in the *Synechocystis* reaction. Subsequent low-temperature Chlide binding experiments have allowed us to propose a scheme for the overall reaction pathway.

MATERIALS AND METHODS

Cloning, Expression, and Purification of POR from Thermosynechococcus elongatus BP-1. The DNA encoding POR was amplified from *T. elongatus* BP-1 genomic DNA by PCR using two sets of oligonucleotide primers, GCCCATATGAGT GATCAGCCACGCCCA and GCCGGATCCTTAGGCCAATCCCACCAG, which were specific to the 5′ and 3′ ends of the coding region. The resulting PCR product was cloned into the pET9-His expression plasmid, and His-tagged POR was overproduced in *Escherichia coli* and purified as previously described (*15*). The enzyme was purified further on a second column (2.5 cm × 10 cm) containing Blue Sepharose 6 Fast Flow (Pharmacia Biotech) equilibrated with 50 mM Tris/HCl (pH 7.5), 1 mM DTT, and 20 mM NaCl. The resin was washed with 10−20 column volumes of this buffer and the His-tagged POR was eluted with 50 mM Tris/HCl (pH 7.5), 1 mM DTT, and 2 M NaCl.

Pigment Preparation. Pchlide was isolated from *Rhodobacter capsulatus* ZY5 cultures as previously described (*18*). The Chlide product was produced by illuminating 50 mL samples containing 20 μM Pchlide, 10 μM POR, and 100 μM NADPH in 50 mM Tris/HCl (pH 7.5), 0.1% (v/v) Genapol X-080, and 0.1% (v/v) β-mercaptoethanol with a Schott KL1500 electronic cold light source (150 μmol m^{-2} s^{-1} white light) for 1 h. The pigment was extracted into diethyl ether, dried under nitrogen, and stored in the dark at −20 °C until required. Before use, the pigment was redissolved in 100% methanol.

Low-Temperature Fluorescence and Absorbance Assays. All spectra were measured in activity buffer [44% glycerol, 20% sucrose, 50 mM Tris/HCl (pH 7.5), 0.1% (v/v) Genapol X-080, and 0.1% (v/v) β-mercaptoethanol], and samples were maintained at the required temperature by use of an OpstistatDN nitrogen bath cryostat (Oxford Instruments). The temperature of the sample was monitored directly with a thermocouple sensor (Comark) and intermediates in the reaction pathway were isolated as previously described (*18*). Fluorescence spectra were recorded on a SPEX FluoroLog spectrofluorometer (Jobin Yvon Ltd.) at 77 K. The exciting light was provided from a xenon light source, with excitation monochromator slit widths of 4.5 nm and emission monochromator slit widths of 3.6 nm. Absorbance spectra were recorded with a Cary 500 Scan UV−visible−NIR (Varian) spectrophotometer at 77 K. Normalization of the spectra, spectral deconvolutions, and difference spectra were calculated by use of the Galactics software.

RESULTS

We have previously identified three distinct steps in the reaction pathway for the *Synechocystis* enzyme, an initial light-driven one (*17*) followed by two dark reactions (*18*). The first dark step resulted in the formation of a new intermediate that has an absorbance maximum at 681 nm (A681, F684) and the second dark step involved a gradual blue-shifting of this state to yield the unbound product, Chlide. In the present work we have studied the dark reactions for the enzyme from the thermophilic cyanobacterium *T. elongatus* by using a combination of low-temperature absorbance and fluorescence measurements. All samples were illuminated at 185 K for 10 min to trigger the initial photochemical step and were then warmed to progressively higher temperatures between 185 and 330 K in the dark. As a result this conversion could be resolved into four separate nonphotochemical steps.

First Dark Step. The first dark step for the thermophilic enzyme is almost identical to the equivalent step for *Synechocystis* POR. Low-temperature absorbance spectra show that the broad absorbance band at 696 nm, which is formed after the initial photochemistry, is converted to the intermediate that absorbs at 681 nm (Figure 1A). Low-temperature fluorescence measurements confirm that this intermediate is the same as the one formed during the *Synechocystis* reaction. The newly formed state has a single fluorescence band at 684 nm (Figure 1A, inset). The temperature dependence of this step, which is obtained by measuring the increase in fluorescence intensity at 684 nm, shows that it is shifted by approximately 5 °C when compared to the *Synechocystis* enzyme (Figure 1B) and can occur between 185 and 215 K.

Second Dark Step. The use of the thermophilic enzyme has revealed new features of the latter stages of the reaction that are not apparent or resolvable for the *Synechocystis* enzyme. Significant differences can be observed between the two enzymes during the second dark step of the reaction. Low-temperature absorbance spectra reveal that the A681 intermediate state does not undergo a gradual blue-shifting to yield the free product, Chlide, as seen in the *Synechocystis*

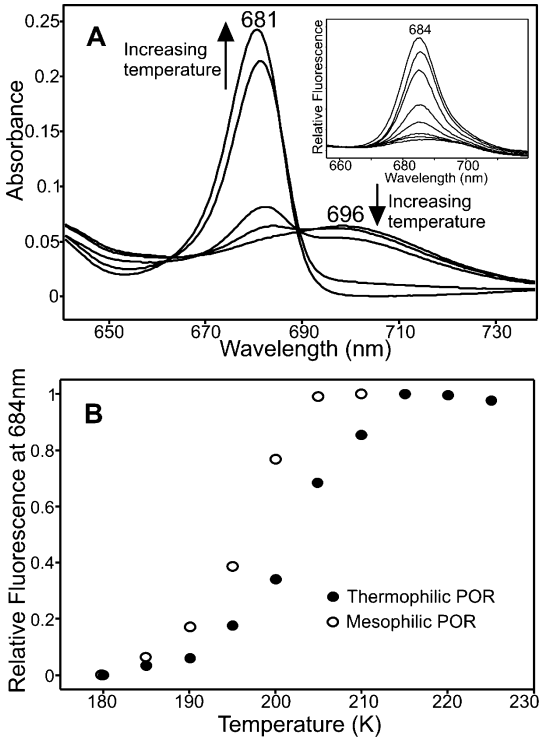

FIGURE 1: Spectroscopic characterization of the first dark step of the reaction catalyzed by thermophilic POR. (A) Absorbance spectra (77 K) of samples containing 3.75 μM Pchlide, 60 μM POR, and 400 μM NADPH after illumination for 10 min at 185 K and incubation in the dark for 10 min at 185, 190, 195, 205, and 215 K. Formation of the absorbance peak at 681 nm and simultaneous disappearance of the broad absorbance band at 696 nm at higher temperatures are indicated by the arrows. (Inset) Fluorescence emission spectra (77 K) of samples containing 1.25 μM Pchlide, 48 μM POR, and 110 μM NADPH after illumination for 10 min at 185 K and incubation in the dark for 10 min at 185, 190, 195, 200, 205, 210, 215, and 220 K. Spectra were recorded with an excitation wavelength of 450 nm and were normalized to the fluorescence of 0.5 μM fluorescein at 500 nm. (B) Temperature dependence of the first dark step was calculated by measuring the relative increase in fluorescence at 684 nm (●) over the temperature range 185−225 K. Temperature dependence of the first dark step for the *Synechocystis* reaction (*17*) is also overlaid (○).

reaction. Instead, the second dark step for the thermophilic enzyme involves the disappearance of the A681 band together with the simultaneous appearance of a new species absorbing at 671 nm (Figure 2A). Deconvolution of this 671 nm peak confirms that it is a single component with a full width at half-maximum (fwhm) of 16 nm. Second derivatives, spectral deconvolution, and difference spectra reveal that all of the intermediate bands consist of a mixture of the 681- and 671-nm bands (Figure 2A, inset) rather than the single components that were observed for the *Synechocystis* enzyme (*18*).

A similar effect is observed when the same step is studied by using low-temperature fluorescence measurements. There is a decrease in the fluorescence band at 684 nm, which is converted into a new fluorescence peak at 674 nm (Figure 2B). Spectral deconvolution of this new band reveals that it consists of a single component with a half-bandwidth of 18 nm. The temperature dependence of this step, which is obtained by measuring the increase in fluorescence intensity at 674 nm, shows that it can occur between 220 and 260 K and is increased by approximately 20 °C when compared to the *Synechocystis* enzyme (Figure 2C).

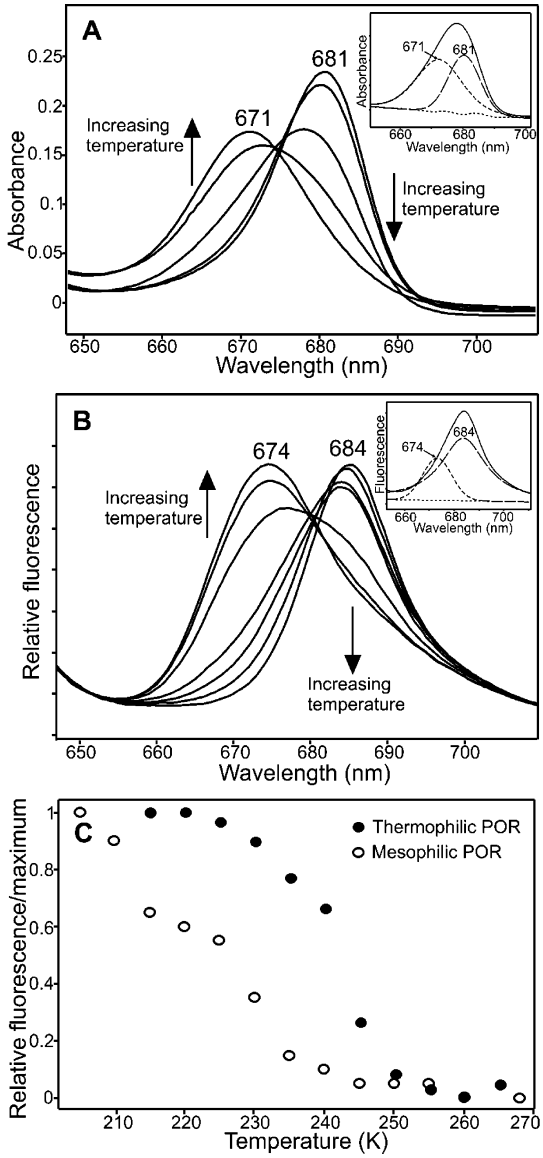

FIGURE 2: Spectroscopic characterization of the second dark step of the reaction catalyzed by thermophilic POR. (A) Absorbance spectra (77 K) of samples containing 3.75 μM Pchlide, 60 μM POR, and 400 μM NADPH after illumination for 10 min at 185 K and incubation in the dark for 10 min at 220, 230, 240, 250, and 260 K. Formation of the absorbance peak at 671 nm and simultaneous disappearance of the absorbance band at 681 nm at higher temperatures are indicated by the arrows. (Inset) Deconvolution of the 240 K spectrum, with the residuals represented by the dotted line. (B) Fluorescence emission spectra (77 K) of samples containing 1.25 μM Pchlide, 48 μM POR, and 110 μM NADPH after illumination for 10 min at 185 K and incubation in the dark for 10 min at 220, 230, 235, 240, 245, 250, and 260 K. Arrows indicate formation of a fluorescence band at 674 nm and disappearance of the fluorescence band at 684 nm at increasing temperatures. Spectra were recorded with an excitation wavelength of 450 nm and were normalized to the fluorescence of 0.5 μM fluorescein at 500 nm. (Inset) Deconvolution of the 245 K spectrum, with the residuals represented by the dotted line. (C) Temperature dependence of the second dark step was calculated by measuring the relative increase in fluorescence at 674 nm (●) over the temperature range 215−265 K. Temperature dependence of the second dark step for the *Synechocystis* reaction (*18*) is also overlaid (○).

Identification of Two Additional Dark Reactions. Although no further spectral changes could be observed after the second dark step for the *Synechocystis* reaction (*18*), the use

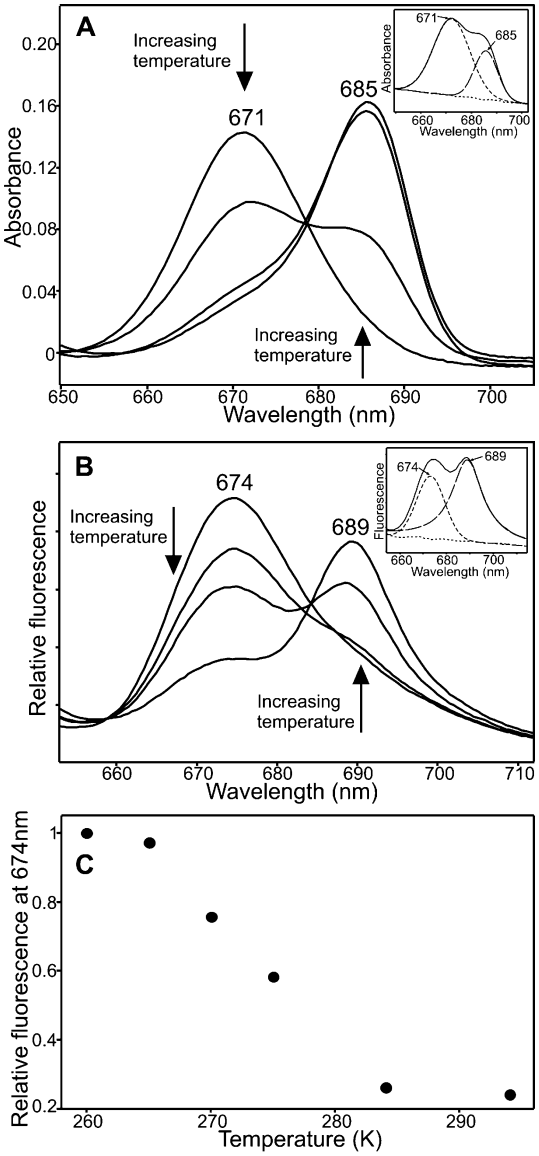

FIGURE 3: Identification of a third dark step in the thermophilic reaction. (A) Absorbance spectra (77 K) of samples containing 3.75 μM Pchlide, 60 μM POR, and 400 μM NADPH after illumination for 10 min at 185 K and incubation in the dark for 10 min at 260, 270, 280, and 290 K. Arrows indicate formation of the absorbance peak at 685 nm together with disappearance of the absorbance band at 671 nm at increasing temperatures. (Inset) Deconvolution of the 270 K spectrum, with the residuals represented by the dotted line. (B) Fluorescence emission spectra (77 K) of samples containing 1.25 μM Pchlide, 48 μM POR, and 110 μM NADPH after illumination for 10 min at 185 K and incubation in the dark for 10 min at 260, 270, 275, and 294 K. Formation of the fluorescence band at 689 nm and simultaneous disappearance of the fluorescence band at 674 nm at higher temperatures are indicated by the arrows. Spectra were recorded with an excitation wavelength of 450 nm and were normalized to the fluorescence of 0.5 μM fluorescein at 500 nm. (Inset) Deconvolution of the 275 K spectrum, with the residuals represented by the dotted line. (C) Temperature dependence of the third dark step was calculated by measuring the relative decrease in fluorescence at 674 nm over the temperature range 260−294 K.

of thermophilic POR has revealed two additional steps, which occur at temperatures above 260 K. The first of these, which now becomes the third dark reaction, involves the conversion of the 671-nm absorbance band into a new state that has an absorbance peak at 685 nm (A685) (Figure 3A). Spectral deconvolution of this new band reveals that it consists of a single component with a half-bandwidth of 13 nm. The equivalent step was also monitored by using 77 K fluorescence measurements (Figure 3B). It involves the disappearance of the fluorescence band at 674 nm together with the formation of the new state, which fluoresces at 689 nm. The new fluorescence band at 689 nm consists of a single component with a fwhm of 15 nm. A temperature dependence of the third dark step can be measured by plotting out the relative fluorescence at 674 nm and reveals that it can occur between 260 and 294 K (Figure 3C).

During the fourth dark step, the A685 state appears to be converted back to a species that has an absorbance band at 671 nm (Figure 4A). Fluorescence spectra at 77 K show that the fluorescence band at 689 nm is also converted back to a state that fluoresces at 674 nm (Figure 4B). A temperature dependence of this fourth dark step has been measured by plotting out the relative fluorescence at 674 nm over a range of temperatures (Figure 4C) and shows that this stage in the reaction can occur at temperatures above 294 K.

Low-Temperature Chlide Binding Experiments. These previously unidentified latter stages are likely to involve Chlide in a series of associations with POR, $NADP^+$, and NADPH. To establish the identity of the spectral forms characterized in Figures 1−4, the product of the reaction, Chlide, was mixed with various combinations of enzyme and cofactor and analyzed by using 77 K fluorescence measurements. Free or unbound Chlide yielded a single fluorescence band at 674 nm (F674) with a fwhm of 18 nm (Figure 5A). The fluorescence maximum and bandwidth remained unchanged in the presence of POR alone. However, inclusion of either of the cofactors NADPH or $NADP^+$ results in the detection of enzyme-bound Chlide species that have red-shifted fluorescence maxima, presumably arising from the formation of a ternary complex. In the presence of $NADP^+$ a shoulder appears at the red edge of the main Chlide band. Difference spectra (Figure 5B) show that this red shift arises from a second Chlide species with a fluorescence maximum at 684 nm (F684). This species was also investigated by spectral deconvolution (data not shown), which yielded a band with a fwhm of 16 nm. When NADPH is used, a new band with a fluorescence maximum at 689 nm (F689) and a fwhm of 15 nm is observed, representing a POR−Chlide−NADPH ternary complex. These same spectral species were also identified when the Chlide binding experiments were repeated for the *Synechocystis* enzyme (data not shown).

DISCUSSION

The reduction of Pchlide to Chlide is catalyzed by the light-driven enzyme POR and is an important reaction in the chlorophyll biosynthetic pathway (*2*). The fact that POR is light-activated means that intermediates in the reaction pathway can be observed by initiating catalysis with illumination at low temperatures. This makes it an important generic model for studying the mechanism of other enzymes in the same protein family as well as enzyme catalysis involving proton and hydride transfers. We have previously used low-temperature fluorescence and absorbance measurements to analyze intermediates in the reaction pathway for the enzyme from *Synechocystis*.

We were able to show that the catalytic mechanism of this enzyme consisted of three separate steps, an initial light-

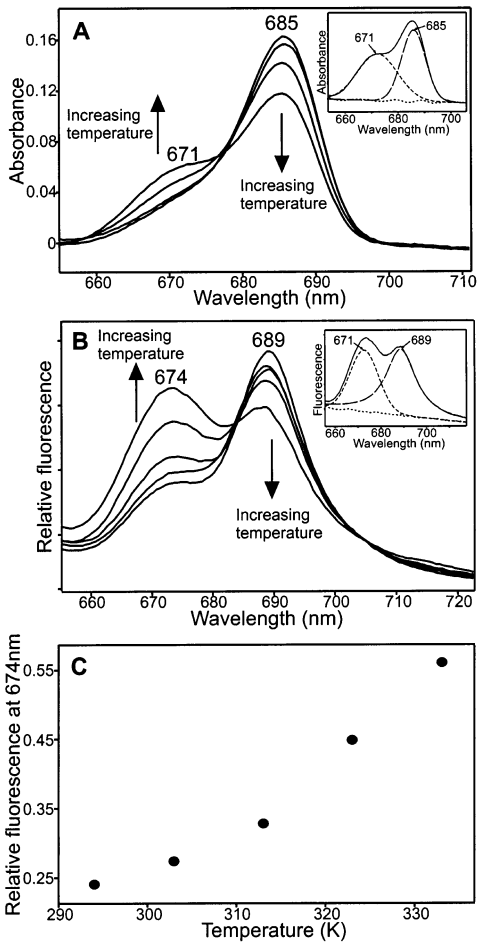

FIGURE 4: Characterization of a fourth dark step in the thermophilic reaction. (A) Absorbance spectra (77 K) of samples containing 3.75 μM Pchlide, 60 μM POR, and 400 μM NADPH after illumination for 10 min at 185 K and incubation in the dark for 10 min at 290, 300, 310, 320, and 330 K. Formation of the absorbance peak at 671 nm and simultaneous disappearance of the absorbance band at 685 nm at higher temperatures are indicated by the arrows. (Inset) Deconvolution of the 330 K spectrum, with the residuals represented by the dotted line. (B) Fluorescence emission spectra (77 K) of samples containing 1.25 μM Pchlide, 48 μM POR, and 110 μM NADPH after illumination for 10 min at 185 K and incubation in the dark for 10 min at 294, 303, 313, 323, and 333 K. Arrows indicate formation of a fluorescence band at 674 nm and disappearance of the fluorescence band at 689 nm at increasing temperatures. Spectra were recorded with an excitation wavelength of 450 nm and were normalized to the fluorescence of 0.5 μM fluorescein at 500 nm. (Inset) Deconvolution of the 333 K spectrum, with the residuals represented by the dotted line. (C) Temperature dependence of the fourth dark step was calculated by measuring the relative increase in fluorescence at 674 nm over the temperature range 294−333 K.

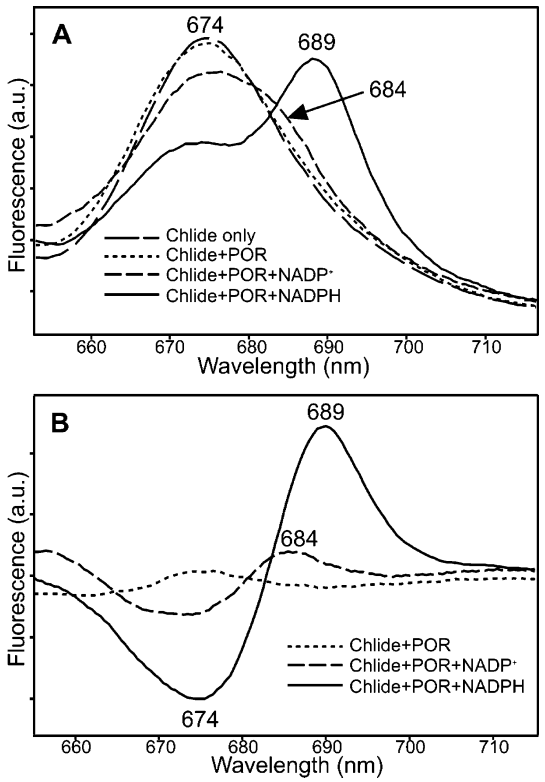

FIGURE 5: Low-temperature fluorescence excitation spectra of free and bound Chlide. (A) Fluorescence emission spectra (77 K) of free Chlide (0.8 μM), Chlide + thermophilic POR (58 μM), Chlide + POR + $NADP^+$ (500 μM), and Chlide + POR + NADPH (200 μM). All spectra were recorded with an excitation wavelength of 450 nm and were normalized to the fluorescence of 0.5 μM fluorescein at 500 nm. (B) Difference spectra of samples from panel A, with the Chlide-only sample as a blank.

driven one that is followed by two dark reactions, each with a distinct temperature dependence. The two dark steps can only occur close to or above the glass transition temperature of proteins, implying a role for protein dynamics during these stages of the reaction (*17*, *18*).

In the present work a thermophilic form of POR has been studied by using low-temperature spectroscopy, and this has provided a much larger temperature range over which to study the reaction. Thermophilic enzymes have also been shown to exhibit a loss of activity at lower temperatures, which has been attributed to an increase in the conformational rigidity at these reduced temperatures (*20*−*22*). Consequently, the thermophilic POR should prove to be an ideal system to study the latter stages of the reaction, where protein motions are proposed to be important. As a result we have observed significant spectral differences during the final stages of the reaction for this enzyme. In the *Synechocystis* reaction the second dark step involves a gradual blue shift and broadening of the absorbance band at 681 nm to yield the unbound product, Chlide (A671). The same phenomenon was also observed in the fluorescence spectra with a blue-shifting of the F684 band, resulting in the formation of free Chlide, and a characteristic fluorescence band at 674 nm (*18*). In the thermophilic enzyme this second dark step differs as the A681−F684 state disappears and is actually converted to a new species, which has an absorbance maximum at 674 nm and a fluorescence maximum at 684 nm. The intermediate bands were shown to consist of a mixture of the two species, unlike the *Synechocystis* enzyme, where a combination of A681 and A671 forms could not be observed (*18*). There is also a large shift in the temperature dependence of this step by approximately 20 °C, which may be caused by a lack of protein flexibility in the thermophilic enzyme at the lower temperatures.

Although the *Synechocystis* reaction appears to be complete after the second dark step (*18*), two additional steps have been identified for thermophilic POR, which can only occur at much higher temperatures. The third dark step involves the conversion of the A671−F674 species to a new state that has an absorbance band at 685 nm and a fluorescence band at 689 nm. This intermediate was not

detected during the *Synechocystis* reaction (*18*) and has not been observed in other low-temperature *in vitro* studies on mesophilic organisms (*14*, *16*). During the fourth dark event of the thermophilic enzyme, the A685−F689 state is converted back to a state that is spectroscopically identical or very similar to the one that had been formed earlier in the reaction (A671−F674). This final step in the reaction pathway only occurs at temperatures greater than room temperature and appears not to have reached completion even at temperatures above 60 °C. In all of the spectral conversions resulting from the dark reactions, the data could be fitted to single starting and finishing components with satisfactory residuals (Figures 2−4). Nevertheless, these spectra do not produce perfect isosbestic points, so it is possible that there are small additional components that are beyond the scope of our analysis.

The binding of the Chlide product to the enzyme in the presence of either of the two cofactors, NADPH and $NADP^+$, causes a significant red shift in the fluorescence emission maximum of the pigment. The degree of this red shift is dependent on the cofactor that is also bound to the enzyme, as we have identified different fluorescent species in the presence of NADPH (F689) and $NADP^+$ (F684). This indicates that interactions between the pigment and the cofactor may play an important role in the shift, and thus in pigment binding. A similar phenomenon could be observed when the Pchlide substrate became bound to the enzyme as the fluorescence maximum was red-shifted by ∼13 nm in the presence of NADPH and ∼10 nm in the presence of $NADP^+$ (*17*).

Previous studies on etioplast membranes have shown that several spectrally distinct forms of the Pchlide substrate and Chlide product can be identified in vivo (*23*−*26*). Moreover, species that are comparable to the Chlide states that we have observed in vitro can be detected in these preparations. However, we do not observe the long-wavelength intermediate, F696, which has been identified in etioplasts and can be attributed to the large POR−NADPH−Chlide aggregates that form only in these membranes (*26*).

As a result of the low-temperature Chlide binding studies, we can identify the states that are formed during the thermophilic reaction. This allows us to propose a reaction scheme for the photoreduction of the ternary enzyme−substrate complex to the final product for both the mesophilic and thermophilic enzymes (Figure 6). The initial light-driven step (data not shown) and the first dark step are almost identical between the two systems and probably represent the chemistry of the reaction resulting in the formation of a POR−$NADP^{+-}$Chlide ternary product complex (A681−F684).

The remaining steps in the reaction can be attributed to a series of product release and cofactor rebinding events. The progressive blue shift that was observed during the second dark step of the *Synechocystis* reaction is likely to be caused by a gradual dissolution of this POR−$NADP^{+-}$Chlide complex to yield the unbound products (*18*). However, in the thermophilic enzyme it would appear that only the $NADP^+$ cofactor is released from the enzyme during the second dark step with the Chlide remaining in a bound state (A671−F674). It is possible that the thermophilic protein is in too rigid a state at these temperatures to surmount the energy barrier for Chlide release, and as a result, Chlide

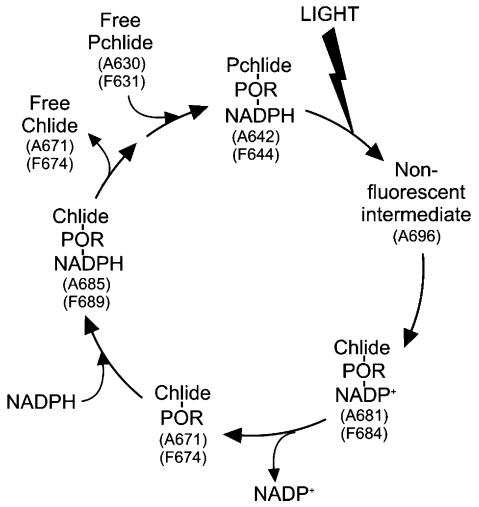

FIGURE 6: Overall scheme for the catalytic cycle of POR. The present work has shown that the Chlide−POR, Chlide−POR−$NADP^+$, and Chlide−POR−NADPH species can exist in both thermophilic and mesophilic enzymes. However, the stepwise formation of these species has only been observed for the thermophilic enzyme, presumably because this system provides an extended thermal range over which these steps in the reaction can be dissected and studied.

remains trapped in the binding pocket. Subsequently, this allows the NADPH substrate to rebind to the enzyme resulting in the formation of a POR−NADPH−Chlide ternary complex (A685−F689). A further increase in thermal energy is required to liberate the Chlide product from the enzyme, giving rise to free pigment (A671−F674), before another Pchlide molecule can bind to initiate a new catalytic cycle. Hence, we have shown that of the two product release steps, $NADP^+$ release has a lower energy barrier to surmount than Chlide release.

In conclusion, we have used a variety of low-temperature spectroscopic studies to isolate the intermediates that are formed during the dark steps of the thermophilic reaction, which has allowed us to propose a mechanism for these events. The whole catalytic cycle presented in Figure 6 shows a proposed order of binding of both substrates and products. This cycle is likely to operate in all PORs, but the separate product release steps cannot be distinguished from one another in the mesophilic enzyme because of the more compressed thermal range over which they occur in comparison to the thermophilic POR.

REFERENCES

1. Griffiths, W. T. (1978) Reconstruction of chlorophyllide formation by isolated etioplast membranes, *Biochem. J. 174*, 681−692.
2. Lebedev, N., and Timko, M. P. (1998) Protochlorophyllide photoreduction, *Photosynth. Res. 58*, 5−23.
3. Fujita, Y., and Bauer, C. E. (2000) Reconstitution of light-independent protochlorophyllide reductase from purified BchL and BchN−BchB subunits−*in vitro* confirmation of nitrogenase-like features of a bacteriochlorophyll biosynthesis enzyme, *J. Biol. Chem. 275*, 23583−23588.
4. Valera, V., Fung, M., Wessler, A. N., and Richards, W. R. (1987) Synthesis of 4*R*- and 4*S*-tritium labeled NADPH for the determination of the coenzyme stereospecificity of NADPH−protochlorophyllide oxidoreductase, *Biochem. Biophys. Res. Commun. 148*, 515−520.
5. Begley, T. P., and Young, H. (1989) Protochlorophyllide reductase. 1. Determination of the regiochemistry and the stereochemistry

of the reduction of protochlorophyllide to chlorophyllide, *J. Am. Chem. Soc. 111*, 3095−3096.
6. Wilks, H. M., and Timko, M. P. (1995) A light-dependent complementation system for analysis of NADPH:protochlorophyllide oxidoreductase. Identification and mutagenesis of two conserved residues that are essential for enzyme activity, *Proc. Natl. Acad. Sci. U.S.A. 92*, 724−728.
7. Griffiths, W. T. (1980) Substrate-specificity studies on protochlorophyllide reductase in barley (*Hordeum vulgare*) etioplast membranes, *Biochem. J. 186*, 267−278.
8. Klement, H., Helfrich, M., Oster, U., Schoch, S., and Rudiger, W. (1999) Pigment-free NADPH:protochlorophyllide oxidoreductase from *Avena sativa* L, *Eur. J. Biochem. 265*, 862−874.
9. Baker, M. E. (1994) Protochlorophyllide reductase is homologous to human carbonyl reductase and pig 20-β-hydroxysteroid dehydrogenase, *Biochem. J. 300*, 605−607.
10. Jörnvall, H., Persson, B., Krook, M., Atrian, S., Gonzalez-Duarte, R., Jeffery, J., and Ghosh, D. (1995) Short-chain dehydrogenases/reductases (SDR), *Biochemistry 34*, 6003−6013.
11. Townley, H. E., Sessions, R. B., Clarke, A. R., Dafforn, T. R., and Griffiths, W. T. (2001) Protochlorophyllide oxidoreductase: A homology model examined by site-directed mutagenesis, *Proteins: Struct., Funct., Genet. 44*, 329−335.
12. Martin, G. E. M., Timko, M. P., and Wilks, H. M. (1997) Purification and kinetic analysis of pea (*Pisum sativum* L.) NADPH:protochlorophyllide oxidoreductase expressed as a fusion with maltose-binding protein in *Escherichia coli*, *Biochem. J. 325*, 139−145.
13. Townley, H. E., Griffiths, W. T., and Nugent, J. P. (1998) A reappraisal of the mechanism of the photoenzyme protochlorophyllide reductase based on studies with the heterologously expressed protein, *FEBS Lett. 422*, 19−22.
14. Lebedev, N., and Timko, M. P. (1999) Protochlorophyllide oxidoreductase B-catalyzed protochlorophyllide photoreduction in vitro: Insight into the mechanism of chlorophyll formation in light-adapted plants, *Proc. Natl. Acad. Sci. U.S.A. 96*, 9954−9959.
15. Heyes, D. J., Martin, G. E. M., Reid, R. J., Hunter, C. N., and Wilks, H. M. (2000) NADPH:protochlorophyllide oxidoreductase from *Synechocystis*: overexpression, purification and preliminary characterization, *FEBS Lett. 483*, 47−51.
16. Lebedev, N., Karginova, O., McIvor, W., and Timko, M. P. (2001) Tyr275 and Lys279 stabilize NADPH within the catalytic site of NADPH:protochlorophyllide oxidoreductase and are involved in the formation of the enzyme photoactive state, *Biochemistry 40*, 12562−12574.
17. Heyes, D. J., Ruban, A. V., Wilks, H. M., and Hunter, C. N. (2002) Enzymology below 200 K: the kinetics and thermodynamics of the photochemistry catalyzed by protochlorophyllide oxidoreductase, *Proc. Natl. Acad. Sci. U.S.A. 99*, 11145−11150.
18. Heyes, D. J., Ruban, A. V., and Hunter, C. N. (2003) Protochlorophyllide oxidoreductase: spectroscopic characterization of the dark reactions, *Biochemistry 42*, 523−528.
19. Heyes, D. J. Hunter, C. N., van Stokkum, I. H. M., van Grondelle, R., and Groot, M. L. (2003) Ultrafast enzymatic reaction dynamics in protochlorophyllide oxidoreductase, *Nat. Struct. Biol. 10*, 491−492.
20. Zavodszky, P., Kardos, J., Svingor, A., and Petsko, G. A. (1998) Adjustment of conformational flexibility is a key event in the thermal adaptation of proteins, *Proc. Natl. Acad. Sci. U.S.A. 95*, 7406−7411.
21. Kohen, A., Cannio, R., Bartolucci, S., and Klinman, J. P. (1999) Enzyme dynamics and hydrogen tunnelling in a thermophilic alcohol dehydrogenase, *Nature 399*, 496−499.
22. Fields, P. A. (2001) Protein function at thermal extremes: balancing stability and flexibility, *Comp. Biochem. Physiol. A 129*, 417−431.
23. Belyaeva, O. B., Timofeev, K. N., and Litvin, F. F. (1988) The primary reactions in the protochlorophyll(ide) photoreduction as investigated by optical and electron-spin-resonance spectroscopy, *Photosynth. Res. 15*, 247−256.
24. Boddi, B., Ryberg, M., and Sundqvist, C. (1992) Identification of 4 universal protochlorophyllide forms in dark-grown leaves by analyses of the 77K fluorescence emission-spectra, *J. Photochem. Photobiol. B—Biol. 12*, 389−401.
25. Boddi, B., Ryberg, M., and Sundqvist, C. (1993) Analysis of the 77K fluorescence emission and excitation-spectra of isolated etioplast inner membranes, *J. Photochem. Photobiol. B—Biol. 21*, 125−133.
26. Boddi, B., and Franck, F. (1997) Room-temperature fluorescence spectra of protochlorophyllide and chlorophyllide forms in etiolated bean leaves, *J. Photochem. Photobiol. B—Biol. 41*, 73−82.

BI049576H